Cholesterol-induced LRP3 downregulation promotes cartilage degeneration in osteoarthritis by targeting SDC4

Chenxi Cao
Peking University Third Hospital
Yuanyuan Shi
Peking University Third Hospital
Zhang Xin
Peking University Third Hospital
Qi Li
Peking University Third Hospital
Jiaohao Zhang
Peking University Third Hospital
Fengyuan Zhao
Peking University Third Hospital
Qingyang Meng
Peking University Third Hospital
Wenli Dai
Peking University Third Hospital
Zhenlong Liu
Institute of Sports Medicine, Beijing Key Laboratory of Sports Injuries, Peking University Third Hospital
https://orcid.org/0000-0001-5541-5535
Duan Xiaoning
Peking University Third Hospital
Jiying Zhang
Institute of Sports Medicine, Beijing Key Laboratory of Sports Injuries, Peking University Third Hospital, 49 North Garden Road, Haidian District, Beijing 100191, PR China
Xin Fu
Institute of Sports Medicine, Beijing Key Laboratory of Sports Injuries, Peking University Third Hospital, 49 North Garden Road, Haidian District, Beijing 100191, PR China
Jin Cheng
Peking University Third Hospital
Hu Xiaoqing
Peking University Third Hospital

Yingfang Ao (aoyingfang@163.com)
Peking University Third Hospital

Article

Keywords: High Cholesterol, Chondrocyte Extracellular Matrix Metabolism, Ras Signaling Pathway, Osteoarthritis Pathogenesis

Posted Date: March 30th, 2021

DOI: https://doi.org/10.21203/rs.3.rs-309414/v1

Version of Record: A version of this preprint was published at Nature Communications on November 21st, 2022. See the published version at https://doi.org/10.1038/s41467-022-34830-4.

Abstract

Emerging evidence suggests that osteoarthritis (OA) is associated with high cholesterol levels. However, the specific mechanism remains unclear. Here, we found that cholesterol metabolism-related gene, LRP3 (low-density lipoprotein receptor-related protein 3) is significantly reduced in high-cholesterol diet mouse's cartilage. By using global *Lrp3*$^{-/-}$ mice in vivo and LRP3 lentiviral vector-transduced chondrocytes in vitro, we identified that LRP3 positively regulated chondrocyte extracellular matrix metabolism, and its deficiency aggravated the degeneration of OA cartilage. Regardless of diet, LRP3 overexpression in cartilage attenuated anterior cruciate ligament transection (ACLT)-induced OA progression in rats. Furthermore, LRP3 knockdown upregulated syndecan-4 (SDC4) expression by activating the Ras signaling pathway. We identified SDC4 as a downstream molecular target of LRP3 in OA pathogenesis. Together, these findings suggest that the cholesterol-LRP3-SDC4 axis plays critical roles in the OA development, and the LRP3 gene therapy may provide a new therapeutic regimen for OA treatment.

Introduction

Osteoarthritis (OA) is the most common form of degenerative arthropathy, with clinical manifestations such as pain, limited mobility, and joint deformities, which seriously affect the patient's ability to work and quality of life[1]. Despite high prevalence and societal impact, the aetiology of OA remains unclear. Previous studies largely believed that OA cartilage degeneration is related to aging[2], trauma[3], and abnormal biomechanics[4]. The existing more evidence shows that metabolic syndrome is associated with an increased risk of OA, especially lipid metabolism[5]. The hypercholesterolemia has been proved to be an independent risk factor for systemic OA[6]. Anomalous homeostasis of cholesterol is also shown to be one of the characteristic features of OA development, with accumulation of cholesterol found particularly in the superficial zone of the cartilage[7]. Meanwhile, several researches demonstrated that OA patients have significantly higher serum levels of low-density lipoprotein (LDL) compared to healthy controls[8, 9]. However, the underlying molecular mechanism of high cholesterol involved in OA cartilage degeneration still unclear and needs to be explored[10].

The low-density lipoprotein receptor-related protein (LRP) family is a group of evolutionary conserved cell surface receptors, involved in the regulation of cholesterol metabolism[11], and has other biological functions as well, including cell signal transduction, synaptic plasticity regulation and cell fate determination[12, 13]. In recent years, studies have found that the LRPs are related to the onset and development of OA[14]. LRP5 has been shown to elevate in OA cartilage, and its haplotype mutations can lead to an increased risk of knee OA in patients[15]. Consistently, *Lrp5* knockout mice have significantly reduced cartilage degeneration compared with wild-type mice[16]. Similarly, heterozygosity for an inactivating mutation of *Lrp6* can also aggravate the progression of OA in mice[17]. LRP3 is one of the LRP family members and expresses in a wide range of human tissues[18]. In contrast to other members of the

LRP family that have been thoroughly studied, the biological function of LRP3 has not been elucidated yet, especially its role in OA.

One of the most important characteristics of OA pathogenesis is cartilage extracellular matrix (ECM) degeneration by matrix-degrading enzymes, including aggrecanases and MMPs[19]. Aggrecanases belong to the ADAMTS family of metalloproteinases, and the degradation of aggrecan by ADAMTS-4 and ADAMTS-5[20]. Recent study showed that syndecan-4 (SDC4) was required for ADAMTS-5 activation in chondrocytes during OA, and played an important role in cartilage ECM degeneration[21]. However, the interaction between cholesterol, LRP3 and SDC4-induced ECM degeneration in OA pathogenesis is unknown. Here, we investigated the functional role of the cholesterol-LRP3-SDC4 axis in OA development in this study. The elucidation of such mechanisms could facilitate the development of new and effective therapeutic targets for the treatment of OA.

Results

High cholesterol aggravates OA cartilage degeneration and downregulates the expression of LRP3 in cartilage

Initially, we collected clinical data of 20 OA patients undergoing total knee replacement (TKA) in Peking University Third Hospital and 20 non-OA patients (meniscal injury as control), including blood total cholesterol (TC), Low-density lipoprotein (LDL), and body mass index (BMI) (supplementary fig. S1). And we found that compared with non-OA patients, TC and LDL were significantly higher in OA patients, accompanied by larger BMI and more metabolic diseases, which indicated that the hyperlipidemia was significantly positively correlated with the development of OA (Fig. 1a). Subsequently, we investigated the impact of high cholesterol on human cartilage explants *in vitro*, using exogenous cholesterol and TNF-α stimulation. Safranin-O and toluidine blue staining showed a significant proteoglycans reduction in response to cholesterol and TNF-α, especially under simultaneous stimulation. Meanwhile, immunohistochemistry (IHC) staining showed that the expression of type II collagen was also significantly reduced (Fig. 1b, c).

To further investigate the impact of cholesterol on the development of OA *in vivo*, we examined whether a high-cholesterol diet (HCD)—compared with a regular diet (RD)—affects ACLT-induced experimental OA in mice (Fig. 1d). We observed that mice fed with an HCD exhibited increased body weight, serum TC and LDL levels. Hot plate tests showed that HCD significantly increased OA-induced pain post-surgery (Fig. 1e). Meanwhile, safranin O-fast green and type II collagen IHC staining showed more severe cartilage degeneration in HCD mice than its RD counterparts 4 weeks after ACLT surgery. And the Osteoarthritis Research Society International (OARSI) scores also showed the same trend (Fig. 1f).

Furthermore, RNA sequencing (RNA-seq) analysis indicated that HCD prominently down-regulated the chondrocytes anabolic genes (*Col2a1, Acan* and *Sox9*), and upregulated the anabolism gene (*Mmp13* and *Adamts5*) (Fig. 1g). Meanwhile, we corroborated the above genes changes in rat chondrocytes under

stimulation of cholesterol *in vitro* (Fig. 1h, i). Interestingly, we found that the expression of cholesterol metabolism-related genes, *Lrp3*, decreased significantly (supplementary Fig. S2). The IHC staining showed decreased expression of LRP3 protein in both HCD mice cartilage and human cartilage explant stimulated with high cholesterol (Fig. 1J-l). At the same time, we confirmed this phenomenon in rat chondrocytes by RT-PCR and western blot analysis (Fig. 1m). In brief, the above data suggest that high cholesterol aggravated the development of OA *in vitro* and *in vivo*, and decreased the expression of LRP3 in cartilage.

The expression of LRP3 is decreased during OA development

In order to further clarify the relationship between the expression of LRP3 and OA, we first collected cartilage tissues from 5 trauma patient (as control) and 5 OA patients. Safranin-O and toluidine blue staining showed that compared with normal cartilage, the surface of OA cartilage displayed severely degenerated and exhibited cracks and fissures, with loss of proteoglycan (Fig. 2a, b). IHC staining confirmed LRP3 protein was down-regulated in OA cartilage (Fig. 2c, d). We next investigated the LRP3 expression in cartilage of various murine OA models. In the ACLT-induced rat OA model, OA was confirmed by safranin O-fast green staining and OARSI score (Fig. 2e, f). Cartilage from ACLT surgery groups exhibited a dramatic reduction in LRP3 expression compared with sham control (Fig. 2g, h). Similar observations were observed in the senescence-induced mouse OA model. Senile Mice were mainly manifested by the degeneration of cartilage surface and the loss of proteoglycans (Fig. 2i, j), while LRP3 protein was significantly reduced compared with younger mice (Fig. 2k, l). Moreover, we found that *Lrp3* and the anabolic genes (*Col2a1, Acan* and *Sox9*) were prominently down-regulated in rat OA chondrocytes induced by IL-1β or TNF-α (Fig. 2m and supplementary Fig. S3b). Immunofluorescence co-staining and western bolt also proved that the protein level of LRP3 was decreased significantly in rat OA chondrocytes model (Fig. 2n and supplementary Fig S3a). These results all confirmed that the expression of LRP3 in chondrocytes was decreased during OA development.

LRP3 positively regulates the metabolism of chondrocytes extracellular matrix

To further identify the biological functions of LRP3 in OA, we constructed LRP3 knockdown (Lv-siLrp3) and overexpression (Lv-Lrp3) lentiviral vectors. Through our preliminary experiments, the most suitable MOI for lentivirus infection of rat chondrocytes was 100 (supplementary Fig. S4a, c). The efficiency of gene knockdown and overexpression was verified by RT-PCR (supplementary Fig. S4b, d). Then, we found that LRP3 knockdown led to decrease *Col2a1, Acan* and *Sox9* mRNA expression in normal rat chondrocytes (Fig. 3a). Western blot analysis also showed a down-regulation expression of COL2A1 and SOX9 protein (Fig. 3b). Furthermore, we also found LRP3 knockdown induced the catabolism of chondrocytes ECM. The proteoglycan content was markedly reduced in the three-dimensional pellet-cultured rat chondrocytes (Fig. 3c). The glycosaminoglycan (GAG) content was also significantly reduced

in plate cultured rat chondrocytes testing by alcian blue staining and dimethylmethylene blue (DMMB) assays (Fig. 3d, e). On the contrary, overexpression of LRP3 in TNF-α-induced rat OA chondrocytes significantly increased the expression of COL2A1, ACAN and SOX9, both at the mRNA level and the protein level (Fig. 3f, g). Safranin O and toluidine blue staining also confirmed that after overexpression of LRP3, the proteoglycan content of OA chondrocyte pellets was increased significantly (Fig. 3h). In addition, the GAG content of OA chondrocytes caused by inflammatory factors had been restored (Fig. 3i, j). Those observations revealed that LRP3 positively regulated the metabolism of chondrocytes ECM.

LRP3 deficiency aggravates the degeneration of knee joint cartilage

We further identified the role of LRP3 in the pathogenesis of OA *in vivo* using Lv-siLrp3-mediated rats OA model and global LRP3 knockout mice (*Lrp3*$^{-/-}$ mice). Intra-articular injection of Lv-siLrp3 resulted in the effective down-regulation of LRP3 in cartilage, caused a loss of cartilage GAG and type II collagen, and led to more serious OA performance compared with vehicle group (supplementary Fig. S5). Furthermore, the *Lrp3*$^{-/-}$ mice were generated and the knockout efficiency was confirmed by PCR screening and IHC staining in various tissues, including cartilage, bone, synovium and meniscus (supplementary Fig. S6). Compared with WT counterparts, more severe ACLT-induced cartilage degeneration was observed in *Lrp3*$^{-/-}$ mice at 4 weeks (supplementary Fig. S8) and 8 weeks (Fig. 3k, l), either in the sham or surgery group. Type II collagen was also decreased in the cartilage of *Lrp3*$^{-/-}$ mice (Fig. 3k, m). Micro-CT 3D reconstruction images revealed that the ectopic osteophytes of *Lrp3*$^{-/-}$ mice were significantly increased, the joints surface were obviously rough and the joint space was reduced (Fig. 3n and supplementary Fig. S8c). In addition, the hot plate test showed that the pain response of *Lrp3*$^{-/-}$ mice was more sensitive than WT mice after surgery (Fig. 3o). What's more, we further compared the OA phenotype between the 12-month-old naturally senile *Lrp3*$^{-/-}$ mice and WT mice. Safranin O-fast green staining showed that proteoglycan was barely expressed in the cartilage of aging *Lrp3*$^{-/-}$ mice, and OARSI scores exhibited more serious OA progression (Fig. 3p). IHC analysis also showed that type II collagen was significantly decreased in *Lrp3*$^{-/-}$ mice cartilage (Fig. 3q). Collectively, the above results revealed that deficiency of LRP3 accelerated both post-injury OA and senescence-induced OA development.

Overexpression of LRP3 in cartilage attenuates OA progression

Next, we sought to investigate whether the overexpression of LRP3 could attenuate the progression of OA *in vivo*. According to the research design, 50μl Lv-Lrp3 (Low dose: 1×10^5 lentiviral particles; High dose: 1×10^6 lentiviral particles) or negative control lentiviral (Lv-con335) was injected into the knee joints once a week for six weeks after ACLT (Fig. 4a). Efficiency of lentiviral infection in the knee cartilage was assessed by LRP3 IHC staining and RT-PCR (Fig. 4b, f). Assessing by safranin O-fast green and IHC staining, we observed that LRP3 overexpression markedly inhibited articular cartilage erosion, rescued the

proteoglycan and type II collagen relative to vehicle-treated ACLT controls (Fig. 4b, d). The OARSI scores also suggested Lv-Lrp3-treated knee joints exhibited milder OA phenotype (Fig. 4c). Functional tests were applied for assessing OA alleviation effect after Lv-Lrp3 treatment. The hot plate and weight bearing tests showed that intra-articular injection of Lv-Lrp3 significantly reduced rats OA-induced pain (Fig. 4e). Furthermore, the RT-PCR showed that the anabolic genes (*Col2a1*, *Acan* and *Sox9*) were up-regulated and the catabolic genes (*Adamts5* and *Mmp13*) were down-regulated after the Lv-Lrp3 injection treatment (Fig. 4f), which was consistent with histological analysis. Then, we used micro-CT to examine the effect of Lv-Lrp3 intra-articular injection on osteophyte formation and subchondral bone remodeling in ACLT rats. The CT images showed that the articular surface of the Lv-Lrp3 injection treatment group was smoother than that of the vehicle treatment group, and the generation of ectopic osteophytes was reduced. Besides, Lv-Lrp3 injection treatment increased the tibial trabecular bone volume per total volume (BV/TV) and decreased the trabecular bone pattern factor (Tb. Pf) compared with vehicle group post ACLT (Fig. 4g). Meanwhile, a nanoindentation test was carried out to determine the biomechanical properties of the rat's articular cartilage. The Lv-Lrp3 injection treatment group exhibited a higher elastic modulus and hardness compared with those in the vehicle-treated group, which were closer to normal cartilage tissue. And the load-depth curve revealed consistent results (Fig. 4h).

Moreover, we performed rescue experiments on *Lrp3*$^{-/-}$ mice after ACLT with Lv-Lrp3 (supplementary Fig. S9a). Efficiency of LRP3 rescue was assessed by LRP3 immunohistochemical staining. The results showed that, after 4 weeks Lv-Lrp3 injection, the OA phenotypes of *Lrp3*$^{-/-}$ mice were significantly attenuated and rescued (supplementary Fig. S9b). The OARSI scores was significantly reduced, and the expression of type II collagen was significantly increased (supplementary Fig. 9c, d). Therefore, we concluded that overexpression of LRP3 attenuated cartilage degradation under OA condition.

Knockdown of LRP3 up-regulates the expression of SDC4 by activating the Ras/Raf/MEK/ERK signaling pathway in chondrocytes

To identify the underlying mechanisms of LRP3 on OA development, we performed RNA-seq analyses in the samples of rat chondrocytes treated with Lv-siLrp3 or Lv-con313. In all, 5903 genes were differentially expressed after *Lrp3* knockdown. Among them, transcripts of 3116 genes were upregulated, whereas 2787 genes were downregulated (Fig. 5b, c). After careful screening, we found that SDC4, which is closely related to OA cartilage degeneration[22], was significantly up-regulated in responded to *Lrp3* knockdown (Fig. 5a). It suggested that SDC4 may be the downstream molecular target of LRP3 in regulating the degeneration process of OA cartilage. Thus, we verified the relationship between LRP3 and SDC4. The IHC staining results showed that the expression of SDC4 was significantly higher in the articular cartilage of *Lrp3*$^{-/-}$ mice than that of wild-type mice (Fig. 5d). Similar results were shown in the cartilage tissue of rats intra-articular injected with Lv-siLrp3 (Fig. 5e). Interestingly, we also found that the ACLT-induced upregulation of SDC4 was suppressed significantly after Lv-Lrp3 injection treatment (Fig. 5f). Meanwhile, we used RT-PCR and western blot to confirm that knocking down LRP3 upregulated the expression of

SDC4 in normal rat chondrocytes (Fig. 5h), while overexpression of LRP3 effectively downregulated the expression of SDC4 in TNF-α-induced rat OA chondrocytes (Fig. 5j). Therefore, we focused on SDC4 in the subsequent experiments.

Moreover, the KEGG pathway analysis revealed that the Ras/Raf/MEK/ERK signaling pathway was obviously activated after knocking down LRP3 (Fig. 5g). Previous research found that the Ras/Raf/MEK/ERK signaling pathway participated in the regulation of inflammatory response, leading to OA cartilage degradation[23]. At the same time, studies had also showed that the phosphorylation of ERK1/2 was inhibited in chondrocytes of *Sdc4*$^{-/-}$ mice[21]. Therefore, we proposed the hypothesis that knocking down LRP3 caused the up-regulation of SDC4 by activating the Ras/Raf/MEK/ERK signaling pathway. Then we performed western blot to verify the hypothesis. The results showed that knocking down LRP3 significantly increased the expression of Ras, Raf and the phosphorylation level of MEK1/2 and ERK1/2, while the SDC4 was also significantly increased simultaneously. Meanwhile, the Ras signaling pathway inhibitor (Salirasib) abolished the upregulation of SDC4 induced by knocking down LRP3 (Fig. 5i). Furthermore, the Ras signaling pathway was obviously activated in the TNF-α-induced rat OA chondrocytes, while overexpression of LRP3 inhibited the activation of Ras signaling pathway and the expression of SDC4 simultaneously (Fig. 5k). In summary, we concluded that LRP3 negatively regulated the expression of SDC4 in chondrocytes through the Ras/Raf/MEK/ERK signaling pathway.

Identification of SDC4 as the downstream molecular targets of LRP3 in chondrocytes

Firstly, we investigated the relationship between the expression of SDC4 and OA. The IHC analysis showed that either in cartilage of OA patients, ACLT-induced post-traumatic rat OA model, or senescence-induced mouse OA model, the expression of SDC4 was higher than that of their control group respectively (Fig. 6a-c). RT-PCR and western bolt demonstrated that SDC4 was also up-regulated in TNF-α and IL-1β induced rat OA chondrocytes (Fig. 6d). Those results all confirmed that the expression of SDC4 was increased during OA progress, which was consistent with previous studies[24]. We next assessed whether SDC4 had a vital role in cartilage ECM degeneration *in vitro* and *in vivo*. We found that when SDC4 was overexpressed in normal rat chondrocytes by infection of Lv-Sdc4, the mRNA expression of *Col2a1* and *Acan* were decreased significantly (Fig. 6e). Simultaneously, to determine if SDC4 promoted ECM degeneration, we measured generation of aggrecan fragments using neoepitope recognizing anti-ARGSVIL antibodies. A significant increase in aggrecan neoepitope generation was detected by western bolt in normal rat chondrocytes by infection of Lv-Sdc4 compared with Lv-con335 (Fig. 6e). Furthermore, knocking down SDC4 in TNF-α-induced OA rat chondrocytes, resulted in an increase of COL2A1 and ACAN and decrease of aggrecan fragmentation (Fig. 6f). Then, to evaluate the SDC4 biological function of cartilage degeneration *in vivo*, Lv-Sdc4 or negative control lentiviral was injected into the knee joints of ACLT-induced rat OA model once a week for 4 weeks (supplementary Fig. S10a). The Lv-Sdc4 injection group showed a more severe OA phenotype, including the loss of proteoglycans and the increase in OARSI scores (supplementary Fig. S10b, c). The IHC staining results also showed the decrease of type II

collagen, accompanied by the increase of ARGSVIL (supplementary Fig. S10b, d and Fig. 6g). Therefore, we concluded that overexpression of SDC4 could aggravate cartilage degradation by breaking down the chondrocyte ECM. Subsequently, we determined whether SDC4 interacted with ADAMTS-5 using co-immunoprecipitation assays. The results showed that after overexpressing of SDC4, pulling down of SDC4 resulted in co-precipitation of more ADAMTS-5 (Fig. 6h). Thus, these data indicated that SDC4 interacted with ADAMTS-5 in the progress of the chondrocyte ECM degeneration. To further explore whether LRP3 regulates the metabolism of cartilage ECM by targeting SDC4, we knocked down LRP3 and SDC4 in normal rat chondrocytes at the same time. The results showed that knocking down SDC4 alleviated the degradation of chondrocyte ECM caused by transfection of Lv-siLrp3 (Fig. 6i). Meanwhile, SDC4 overexpression counteracted ECM catabolism induced by upregulation of LRP3 in TNF-α-induced rat OA chondrocytes (Fig. 6j). In light of these data, we concluded that LRP3 regulates the metabolism of cartilage ECM by targeting SDC4.

Discussion

In this paper, we have made several key observations presented here. (1) Stimulation of high cholesterol can cause disorder of cartilage ECM metabolism *in vitro* and *in vivo*, leading to cartilage degradation, and then aggravating the progression of OA. During this process, the expression of cholesterol metabolism-related gene, LRP3, was significantly reduced in chondrocytes. (2) The expression of LRP3 is downregulated in degenerated human OA cartilage and various murine models of OA. *Lrp3* gene deletion will aggravate cartilage degeneration, while overexpression of LRP3 can suppress the cartilage ECM degeneration, thereby inhibiting the progression of OA. (3) Knockdown of LRP3 can upregulate the expression of SDC4 by activating the Ras/Raf/MEK/ERK signaling pathway in chondrocytes. And the overexpression of SDC4 induced the cartilage ECM degeneration through binding and activating ADAMTS-5. Thus, we proposed that cholesterol-LRP3-SDC4 axis play an important role for the maintenance of cartilage homeostasis and treatment for OA (Fig. 6k).

OA is the most prevalent chronic joint disease mainly affects individuals over the age of 65[25]. Although several risk factors related to OA have been pointed out, including aging, gender, muscle strength, obesity and mechanical alignment[1], the pathogenesis of OA remains largely unclear. In recent years, a large number of epidemiological and basic researches have shown that metabolic syndrome, which is dominated by abnormal cholesterol metabolism, is closely associated with the occurrence and development of OA[26, 27]. A cohort study on knee OA showed that hyperlipidemia is associated with joint pain and an increased prevalence of OA[28]. The pain and OA severity scores of OA patients with hypercholesterolemia were also higher than those of the control group[29]. In this study, we found that serum TC and LDL in patients with OA were significantly higher than that of non-OA patients, which also verified the positive correlation between clinical hyperlipidemia and OA. As for basic research, both $ApoE^{-/-}$ mice and rats fed with HCD were proved to have severity of OA phenotype[30, 31], which was consistent with our study. In addition, we used exogenous cholesterol to stimulate human cartilage explants *in vitro*, and the results showed a significant proteoglycans and type II collagen reduction.

Similarly, Saba Farnaghi *et al.* also found the same change trend when stimulating bovine cartilage explants with cholesterol[30]. Furthermore, studies showed that administration of atorvastatin can reduce the serum cholesterol level while effectively delaying the progression of OA[32]. Statin drugs can also play a similar role in human OA treatment[33]. These results all support the notion that high cholesterol make a significant contribution to the development, progression, and severity of OA. However, the molecular mechanism of cholesterol-induced OA cartilage degeneration has not yet been completely eliminated.

Cholesterol is an important composition ingredient of cartilage cell membrane lipid dual molecular layer, participating in cartilage cell membrane steady state maintenance, cell signal transduction, immune response activation and material transport, and the normal metabolism of cholesterol plays an important role in maintaining cartilage ECM metabolic balance[7, 34, 35]. However, when an abnormal cholesterol metabolism occurs, a series of pathophysiological changes in cartilage cells can be induced, thereby promoting the development of OA. A previous study found that abnormal cholesterol metabolism can lead to cholesterol accumulation in chondrocytes, causing damage to the structure and function of mitochondria, activating the MAPK inflammatory signaling pathway, leading to irreversible damage to chondrocytes and causing cartilage degeneration[30]. Excess cholesterol can also be swallowed by synovial macrophages in the joint chamber, resulting in the accumulation of OX-LDL in macrophages, causing an ectopic bone formation and aggravating OA progression[36]. At the same time, researchers also found that cholesterol hydroxylase CH25H and CYP7B1 were significantly up-regulated in OA chondrocytes, which mediated ECM degradation by promoting the expression of cartilage ECM degrading enzymes MMP-3, MMP-12 and ADAMTS-5[31]. In our research, in order to further explore the molecular mechanism of cholesterol-induced OA cartilage degeneration, we performed RNA-seq on mice OA cartilage tissue induced by feeding with HCD, and found that the expression of LRP3 was significantly reduced. The same result also appeared in the rat OA chondrocyte model stimulated by exogenous cholesterol. This indicates that LRP3 may be a brand-new target in cholesterol-induced OA cartilage degeneration.

As a member of the LRP family, LRP3 was first reported by Hirofumi Ishii et al. in 1998[18]. The human *LRP3* gene was mapped to chromosome bands 19q12-q13.2 and detected in a wide range of human tissues, with the highest expression in skeletal muscle and ovary. In addition to its involvement in lipid metabolism, research on LRP3 is very limited, and its biological function is still unclear[37]. Only one research showed that LRP3 maybe the target of microRNA-4739 in regulation osteogenic and adipocytic differentiation of immortalized human bone marrow stromal cells[38]. In our research, we found that in addition to the decreased expression of LRP3 in cholesterol-induced OA models, it was also downregulated in OA patient cartilage, ACLT-induced rats OA models, senescence-induced mice OA models and inflammatory factors-induced OA chondrocyte models. This indicated that LRP3 itself also played an important biological function in the pathogenesis of OA. Then, we used LRP3 knockdown and overexpression lentiviral vectors and *Lrp3*$^{-/-}$ mice to confirm that LRP3 can regulate the cartilage ECM metabolism, thereby regulating the process of OA cartilage degeneration. More importantly, we have confirmed that overexpression of LRP3 can effectively delay the severity of OA through intra-articular

injection. Therefore, our research not only expands the biological functions of LRP3 in OA, but also provides a new target for the treatment of OA.

Through RNA-seq analysis, we found that the expression of SDC4 was significantly increased after knocking down LRP3 in chondrocytes. We further found that knockdown of LRP3 up-regulated the expression of SDC4 by activating the Ras/Raf/MEK/ERK signaling pathway. As a polysaccharide of heparan sulfate transmembrane transporter, the high expression of SDC4 is closely related to OA cartilage degeneration[22, 39, 40]. Barre *et al*. first discovered that SDC4 mRNA levels were significantly increased in cartilage severe damage zone compared with normal area[39]. Frank *et al*. found that SDC4 was significantly increased in mouse OA cartilage and caused cartilage degeneration by binding and activating ADAMTS-5[21]. These results also have been confirmed in our research. More importantly, through the dual gene intervention of LRP3 and SDC4, we identified that SDC4 as the downstream molecular target of LRP3 in regulation of the cartilage ECM metabolism. To date, we constructed a new interaction between cholesterol, LRP3 and SDC4 in OA pathogenesis.

The current study has several limitations. First, when we studied the downstream molecular mechanism of LRP3, we only searched the gene changes in chondrocytes caused by LRP3 knockdown, but did not study the gene changes caused by overexpression of LRP3, which may ignore some other molecular targets. Second, we only used small animal models to study LRP3 therapeutic effects of OA, the effect of LRP3 on large animals needs to be further investigated. We will continue to study these contents deeply in the future.

In conclusion, we found that high cholesterol inhibited the expression of LRP3 in chondrocytes, triggering an imbalance in cartilage ECM metabolism, leading to the development of OA cartilage degeneration. Among them, SDC4 acted as a downstream molecular target of LRP3 to regulate chondrocytes ECM degeneration. And targeted overexpression of LRP3 can efficiently delay the degeneration of OA cartilage. In brief, the cholesterol-LRP3-SDC4 axis plays a vital role in OA pathogenesis and may provide a new therapeutic avenue for treating OA.

Materials And Methods

Clinical specimen preparation and collection

The clinical data of the patients (n=40), including BMI, Total cholesterol (TC), Low-density lipoprotein (LDL) etc., were obtained from the Department of Sports Medicine, Peking University Third Hospital. Human OA cartilage samples (n=20, 14 females and 7 males with mean age of 64.7 years) were excised from patients undergoing total knee replacement (TKA). Normal human cartilage samples (n=5, 2 females and 3 males with mean age of 53.3 years) were isolated from the knee joints of donors of trauma patients. All protocols were approved by the Ethics Committee of Peking University Third Hospital (PTTH-MEC-SOP-08-1.0-A02). Informed consent was obtained from all patients. The cartilage samples were used for subsequent histological and immunohistochemical assessments.

High-cholesterol diet (HCD) and surgically-induced OA in C57BL/6 mice model

In this study, a surgically-induced OA model used generated using the anterior cruciate ligament transplantation (ACLT) protocol. All animal experimental procedures were approved by the Experimental Animal Ethics Committee of Peking University Third Hospital. A total of 20 wild-type male C57BL/6 mice (five weeks old) were provided by Beijing Vital-River Laboratory Animal Technology Company and maintained in a specific pathogen-free (SPF) environment. Ten mice were fed an AIN-93G diet (Beijing Keao Xieli Feed Co., Ltd., Beijing, China) as the regular diet (RD), while the remaining were fed a modified AIN-93G diet supplemented with 2% cholesterol as a high-cholesterol diet (HCD). After seven weeks on respective diets, ACLT surgery was performed on their right knees and sham surgery was performed on the left knees. Briefly, under general anaesthesia, the joint capsule was cut off, and the anterior cruciate ligament of the right knee was transected. The sham operation on the contralateral knee did not involve ligament transection. The mice were sacrificed four weeks after ACLT/sham surgery for further analysis.

Primary rat chondrocyte isolation and culture

Primary rat chondrocytes were isolated from cartilage fragments dissected from the femoral heads of 6-week-old Sprague–Dawley (SD) rat. The rat cartilage fragments were mechanically sliced into 2–5 mm^3 pieces and enzymatically digested with 0.2% type II collagenase (Gibco, CA, USA) at 37 °C for 6 h. After digestion, cartilage fragment solutions were centrifuged at 1000 rpm for 3 min, and the cells were resuspended in Dulbecco's modified Eagle's medium (DMEM; Gibco) with 10% (v/v) foetal bovine serum (FBS; HyClone, Logan, UT, USA) containing 1 g/L penicillin–streptomycin (Invitrogen, CA, USA) at 37 °C in a humid environment with 5% CO_2.

Chondrocytes were starved for 6 h without FBS and subsequently treated with IL-1β (10 ng/mL; 211-11B; PeproTech, Beijing, China) or TNF-α (20 ng/mL; 315-01B; PeproTech) for 6–48 h according to different experimental requirements.

Cholesterol intervention of cartilage/chondrocytes *in vitro*

Exogenous cholesterol was delivered to the cartilages/chondrocytes using the cholesterol:methyl-b-cyclodextrin (Chol:MbCD) complex (#SLCB4694; Sigma-Aldrich, MO, USA), which makes cholesterol water-soluble and is widely used to successfully deliver cholesterol in a variety of cell types. Human articular cartilage disks were treated with Chol:MbCD complex (50 μg/mL) and/or TNF-α (20 ng/mL) for 14 d. Similarly, primary p1 rat chondrocytes were treated with Chol:MbCD complex (50 μg/mL) and/or TNF-α (20 ng/mL) for 3 d (RNA extraction) or 5 d (protein extraction). Chondrocytes incubated with phosphate-buffered saline (PBS, vehicle) without Chol:MbCD treatment served as controls.

RNA extraction and real-time qPCR

Total RNA was extracted from primary cultured chondrocytes using TRIzol reagent (Invitrogen, Carlsbad, CA, USA). Purified RNA (2 μg) was reverse-transcribed using a RevertAid First Strand cDNA Synthesis Kit (Thermo Fisher Scientific, Boston, MA, USA). Real-time qRT-PCR was performed using the Applied Biosystems StepOnePlus Real-Time PCR System (Foster City, CA, USA) with SYBR Green PCR Master Mix (Toyobo, Japan). Target mRNA expression levels were normalised to that of 18S ribosomal RNA (Rn18s). The relative gene expression was calculated using $2^{-\Delta\Delta CT}$ method and expressed as fold-change. Each RT-qPCR was performed in triplicate, with at least three different biological replicates. The primer sequences were as follows:

Gene name		Sequences
Rn18s	F	5'- GTAACCCGTTGAACCCCATT -3'
	R	5'- CCATCCAATCGGTAGTAGCG -3'
Col2a1	F	5'- CACCGCTAACGTCCAGATGAC -3'
	R	5'- GGAAGGCGTGAGGTCTTCTGT -3'
Acan	F	5'- CATTCGCACGGGAGCAGCCA -3'
	R	5'- TGGGGTCCGTGGGCTCACAA -3'
Sox9	F	5'- TCCCCGCAACAGATCTCCTA -3'
	R	5'- AGCTGTGTGTAGACGGGTTG -3'
Mmp13	F	5'- CTGCGGTTCACTTTGAGGAC -3'
	R	5'- ACAGCATCTACTTTGTCGCC -3'
Adamts5	F	5'- CACGACCCTCAAGAACTTTTGC -3'
	R	5'- TCACATGAATGATGCCCACATAA -3'
Lrp1	F	5'- GGTCCTGAACTGAATCACGCCTTC-3'
	R	5'- TAGACACTGCCGCTCCGATACTC-3'
Lrp2	F	5'- CACCTCCTTCACCTGCGACAATC-3'
	R	5'- CATCCGAGCCATCCGAGCAATC-3'
Lrp3	F	5'- TGGGATGGCTGAACCACAGA -3'
	R	5'- CAGTGGGAAGTTAACAGCA -3'
Lrp4	F	5'- ACACGCTGCTACTGAACAACCTG-3'
	R	5'- GACACCACCTCCTCCACATTGC-3'
Lrp5	F	5'- CTTCATCCACCGTGCCAACCTG-3'
	R	5'- TCTGCCAGTCTGTCCAGTAGAGTG-3'
Lrp6	F	5'- GCCATCCGTCGCTCCTTCATTG-3'
	R	5'- GCCACCCAGTCAACAGCAATACC-3'
Sdc4	F	5'-TGTTGCTCCTCGGAGGTTTC-3'
	R	5'-GGAACCCGACAGCTCAAAGT-3'

Protein extraction and western blot analysis

Chondrocytes were lysed in radioimmunoprecipitation assay (RIPA) lysis buffer containing protease inhibitors and/or a phosphatase inhibitor cocktail. The total cell lysates were prepared in lysis buffer (150 mM NaCl, 1% Nonidet P-40, 50 mM Tris, 5 mM NaF), separated by SDS polyacrylamide gel electrophoresis (PAGE), and transferred to a polyvinylidene fluoride (PVDF) membrane. After blocking with 5% non-fat dry milk in 0.1% Tween 20 TBS (TBST), the membranes were incubated with the corresponding primary antibodies overnight at 4 °C. After washing three times with TBST, the membranes were incubated with secondary antibodies at 21 °C for 1 h and visualised using the BIO-RAD ChemiDoc XRS+ system.

Proteins were analysed using antibodies against COL2A1 (ab34712; Abcam, CA, USA; 1:1000), and GAPDH (TA-08; Zsjqbio, China; 1:1000), SOX9 (ab185966; Abcam; 1: 2000), LRP3 (PA5-50051; Invitrogen, USA; 1:500), SDC4 (ab74139; Abcam; 1:1000), Ras (#3965; Cell Signaling Technology, USA; 1:1000), c-Raf (#9422; Cell Signaling Technology; 1:1000), phospho-Erk1/2 (#4370; Cell Signaling Technology; 1:1000), ERK1/2 (#4695; Cell Signaling Technology; 1:1000), phospho-MEK1/2 (#9154; Cell Signaling Technology; 1:1000), MEK1/2 (#9422; Cell Signaling Technology; 1:1000), VAGSVIL (ab3773; Abcam; 1:1000), and Adamts-5 (ab41037; Abcam; 1:1000). Anti-mouse and anti-rabbit secondary antibodies were purchased from ZSGB-BIO (Beijing, China; 1:1000).

Histology and immunohistochemistry (IHC) assessment

Human cartilage samples were fixed in 4% neutral-buffered paraformaldehyde (PFA; Solarbio, Beijing, China), embedded in paraffin, and sectioned continuously (6-μm thick). The cartilage sections were stained with safranin O (Solarbio) for 5 min and toluidine blue (Solarbio) for 30 min, washed three times with PBS, dried, and mounted.

The excised whole knee joints of rats/mice were fixed in 4% neutral-buffered PFA for 3 d. The specimens were then decalcified for 2 d in a decalcification solution (ZLI-9307; ZSGB-BIO) and dehydrated in a graded ethanol series. Thereafter, the samples were embedded in paraffin, cut into 6-μm thick sections, and stained with Modified Safranin O-Fast Green FCF cartilage Stain Kit (#G1371; Solarbio) according to manufacturer's instructions. Three blinded observers scored the histopathological changes in osteoarthritic cartilage using the Osteoarthritis Research Society International (OARSI) grading system.

For immunohistochemical staining (IHC), the paraffin-embedded sections were incubated with 3% H_2O_2 for 15 min to inhibit endogenous peroxidase, followed by incubation with 10% goat serum for 1 h at 21 °C to block non-specific antigens. Next, the sections were incubated with specific primary antibodies against COL2A1 (ab34712; Abcam; 1:100), LRP3 (human: ab115197; Abcam; 1:50) (rat/mouse: TA323023; Origene, USA; 1:50), and SDC4 (ab74139; Abcam; 1:50), and VAGSVIL (ab3773; Abcam; 1:50) overnight at 4 °C. Subsequently, the sections were incubated for 1 h at 21 °C with horseradish peroxidase-conjugated

secondary antibodies (ZSGB-BIO). The integrated optical density (IOD) value of positive staining was evaluated using ImageJ software (National Institutes of Health, MD, USA). The positive and negative controls for all antibodies are provided in figure S11.

Immunofluorescence analysis

TNF-α- and IL-1β-treated rat chondrocytes were rinsed in PBS and then fixed with 10% neutral-buffered formalin for 30 min at 21 °C. Cells were incubated with Triton X-100 (Beyotime Biotechnology, Beijing, China) for 10 min to penetrate the cell membrane and donkey serum (Beyotime Biotechnology) for 1 h to block nonspecific binding sites. Cultured cells were incubated with primary antibodies against type II collagen (ab34712; Abcam; 1:100), SOX9 (ab185966; Abcam; 1:100), and LRP3 (sc-373736; Santa Cruz Biotechnology, USA; 1:50) at 4 °C overnight. The cells were then washed with PBS three times and incubated with Alexa Fluor 488-conjugated goat anti-rabbit or Alexa Fluor 594-conjugated goat anti-mouse secondary antibodies (Thermo Fisher Scientific; 1:200) for 1 h at 21 °C. Nuclei were stained with DAPI (Beyotime Institute of Biotechnology, Jiangsu, China) for 10 min. Finally, the samples were rinsed with PBS and visualised using a confocal microscope (Olympus Life Science, Tokyo, Japan).

Lentivirus construction and transfection

Lentiviral particles expressing rat/mouse LRP3 (Lv-Lrp3), rat SDC4 (Lv-Sdc4), rat LRP3 knockdown shRNA (Lv-siLrp3), rat SDC4 knockdown shRNA (Lv-siSdc4), and negative control lentiviruses (Lv-con335 and Lv-con313) were purchased from GeneChem Co. Ltd. (Shanghai, China). To construct Lv-Lrp3 and Lv-Sdc4, the mouse LRP3 (NM_001024707), rat LRP3 (NM_053541), and SDC4 (NM_012649) coding regions were cloned into GV492 vectors. The LRP3-GV492 and SDC4-GV492 vectors were mixed with pHelper 1.0 and pHelper 2.0 plasmids, and then co-transfected into HEK-293T cells with Lipofectamine^{TM} 2000 (Invitrogen, Shanghai, China) according to the manufacturer's instructions. After 48-h transfection, viral supernatants were collected, filtered through 0.45-μm polyvinylidene fluoride membranes, and then centrifuged. The lentivirus vector system for packaging Lv-siLrp3 and Lv-siSdc4 was composed of pGCSIL-GFP vector, stably expressing shRNA and a marker (GFP fusion protein), pHelper 1.0 (gag/pol element), and pHelper 2.0 (VSVG element). The shRNA targeting rat *LRP3* (5'-CACCAACTGCAGCTGGTACAT-3'; 5'-AGGCAGTTTCTACGGTTCCTT-3'; 5'-ATGCGGACTGCTGCTTGTTAT-3'), rat *SDC4* (5'-ACCCTTGGTGCCACTAGATAA-3'; 5'-AGGCAGTTACGACTTGGGCAA-3'; 5'-TCGGGTTCCGGAGATCTAGAT-3'), and control shRNA used as a negative control (5'-TTCTCCGAACGTGTCACGT-3') were designed, synthesised, and cloned into the pGCSIL-GFP vector by GeneChem Co. Ltd. The pGCSIL-shRNA-GFP, pHelper 1.0, and pHelper 2.0 were mixed and transfected into 293T cells using Lipofectamine^{TM} 2000 according to the manufacturer's instructions. After 48-h transfection, viral supernatants were collected, filtered through 0.45-μm polyvinylidene fluoride membranes, and centrifuged.

Chondrocytes (50% confluent) were transduced with lentiviral particles at a multiplicity of infection (MOI) of 100. Culture media were replaced with normal media without lentivirus 24 h after transduction. After 3 d, the green fluorescence in the cells was observed using a fluorescence microscope (Olympus Life Science, Tokyo, Japan). At >80% positive fluorescence rate and >90% cell viability, cellular mRNA and proteins were extracted for further analysis.

Pellet culture of rat chondrocytes

Normal rat chondrocytes were transfected with Lv-con313 and Lv-siLrp3 for 3 d. The TNF-α-induced OA rat chondrocytes were transfected with Lv-con335 and Lv-Lrp3 for 3 d. Then, 1×10^6 chondrocytes from each group were added to 15-mL polypropylene conical tubes and centrifuged at 400 g for 5 min to form a cell pellet. The cells were re-suspended in chondrogenic low-glucose DMEM supplemented with 10 ng/mL recombinant human transforming growth factor-beta 3 (Cyagen Biosciences Inc., Santa Clara, CA, USA). The culture media were changed every two days. After 2 weeks of culture, the pellets were harvested for histological assessment.

Alcian blue staining and glycosaminoglycans (GAG) content analysis

After lentiviral transfection, rat chondrocytes were fixed in 4% neutral-buffered PFA for 15 min and then stained with Alcian blue (Cyagen Biosciences Inc.) for 30 min according to the manufacturer's protocol. The total GAGs extracted from the chondrocytes were measured using the 1,9-dimethylmethylene blue (DMMB; Sigma-Aldrich) colorimetric assay. The chondrocyte samples in 96-well plates (n=4 per group) were digested with papain lysates (20 μL) at 65 °C for 1 h and diluted in DMMB working solution (200 μL). Absorbance was then measured at 525 nm using a microplate spectrophotometer (Multiskan Sky, Thermo Fisher Scientific). The proteoglycan content in each sample was calculated based on a standard curve generated using serial dilutions of chondroitin sulfate (Sigma-Aldrich).

C57BL/6-Lrp3 global knockout mice ($Lrp3^{-/-}$ mice)

A total of 90 C57BL/6-Lrp3 global knockout mice ($Lrp3^{-/-}$ mice) were purchased from Cyagen Biosciences, Inc. (Jiangsu, China) and were created by CRISPR/Cas9-mediated genome engineering. Eight exons of *Lrp3* (NM_001024707; Ensembl: ENSMUSG00000001802) were identified, with the ATG start codon in exon 1 and the TGA stop codon in exon 8 (Transcript: ENSMUST00000122409). Exons 4–7 were selected as the target sites. Then, Cas9 and gRNA were co-injected into fertilised eggs to generate $Lrp3^{-/-}$ mice. The pups were genotyped using PCR, followed by sequencing analysis.

OA was induced by ACLT in the 8-week-old male wild-type C57BL/6 or Lrp3$^{-/-}$ mice as described previously. The ACL of the right knee was transected and confirmed by a positive anterior drawer test result. Knee samples were harvested at 4 and 8 weeks after ACLT or sham operation. To study naturally occurring OA, Lrp3$^{-/-}$ mice were raised for 12 months (senescence-induced OA model). To evaluate the gene rescue effect on the Lrp3$^{-/-}$ ACLT-induced OA model, either 20 μL Lv-Lrp3 or Lv-con335 (1×10^6 lentiviral particles) was injected into the knee joints once a week for four weeks. The wild-type and knockout mice were sacrificed for further analyses. All animal experiments were approved by the Animal Care and Use Committee of Peking University Health Science Center and were conducted in compliance with their guidelines.

Intra-articular delivery of lentivirus in SD rat OA model

Intra-articular injections of lentiviral particles were administered 14 d after ACLT in 8-week-old male SD rats. To study the effect of local *LRP3* knockdown in the knee joint cavity of ACLT-induced OA rat model, 50 μL Lv-siLrp3 or Lv-con313 (1×10^6 lentiviral particles) was injected into the knee joints once a week for four weeks. To evaluate the therapeutic effect of upregulated LRP3 expression in the cartilage of these rats, 50 μL Lv-Lrp3 (low dose: 1×10^5 lentiviral particles; high dose: 1×10^6 lentiviral particles) or Lv-con335 (1×10^6 lentiviral particles) was injected into the knee joints once a week for six weeks. Similarly, to evaluate the effect of local upregulation of cartilage SDC4 expression, 50 μL Lv-Sdc4) or Lv-con335 (1×10^6 lentiviral particles) was injected into the knee joints once a week for four weeks. Rats were sacrificed one week after the last injection. The protocol was approved by the Animal Care and Use Committee of the Peking University Third Hospital. The experiments were conducted in accordance with appropriate international guidelines and all relevant ethical regulations for animal testing and research.

Hot plate test

The pain response in the joints of rats/mice in different experimental groups were evaluated by hot plate test. Briefly, the animals were placed on a hot plate meter (Ugo Basile SRL, Italy) at 55 °C, and the time from the point when both hind limbs touched the hot plate until appearance of hind limb responses, such as shaking, jumping, or licking, was measured. Each animal was tested three times with 15 min intervals, and the average of the three response times was considered as the final pain threshold of the rat/mouse. The observers were blinded to the experimental treatments.

Weight bearing test

The weight distribution of hind paws of rats was measured using an incapacitance tester (Ugo Basile SRL). The rats were placed in the detection chamber, and the left and right hind paws were placed on the pressure sensor for 9 s, after which the pressure transducer data were read. The results are shown as the difference between the weight placed on the contralateral sham (left) and the ACLT (right) hind limb. The tests were performed three times for each rat. The observers were blinded to the experimental treatments.

Nanoindentation analysis

Biomechanical characteristics of rat knee cartilage tissue were analysed using an in situ nanomechanical test system (TI-900 TriboIndenter, Hysitron, Minneapolis, MN, USA). Cartilage samples were collected from femoral condyles of the sham, vehicle, and Lv-Lrp3-treated (low and high dose) ACLT-induced OA rat groups (n = 5/group) at 6 weeks. PBS solution was used to maintain cartilage hydration. The indentation cycle consisted of a 10 s peak load, 2 s hold, and 10 s unload. The maximum indentation depth is 2000 nm. The hardness and elastic modulus were determined from the load-depth curve.

Micro-computed tomography (CT) analysis for knee joints

Osteophyte development and subchondral bone remodelling in rats/mouse knee joints was evaluated by micro-CT. The ACLT-induced OA model rats were sacrificed at the designated time points, and intact knee joints, were excised from the surrounding soft tissue (skin and muscles). Samples (n = 4 per group) were scanned using micro-CT (Siemens Inveon MM Gantry, Berlin, Germany) at an isotropic resolution of 5 μm^3. A three-dimensional (3D) model was constructed using Mimics Research software. Histomorphometric analysis was performed on longitudinal images of the tibial subchondral bone, which was also analysed using the Inveon Research Workplace software (Siemens Inveon MM Gantry, Berlin, Germany), determining the trabecular ratio of bone volume to tissue volume (BV/TV) and trabecular bone pattern factor (Tb. Pf.).

RNA sequencing (RNA-seq) for the chondrocyte/cartilage transcriptome

We performed mouse knee cartilage tissue and rat chondrocyte RNA-seq analysis using the NovelBrain Cloud Analysis Platform. Cartilage tissues were collected from the medial and lateral femoral condyles of wild-type C57BL/6 mice on RD or HCD after seven weeks. Rat chondrocytes and control group were transfected with Lv-siLrp3 and Lv-con313 (empty vector), respectively. After 3-d transfection, total RNA was extracted from the rat chondrocytes and cartilage tissue using TRIzol reagent. cDNA libraries were constructed for each pooled RNA sample (rat and mice) using VAHTSTM Total RNA-seq (H/M/R). Differential gene and transcript expression analyses were performed using TopHat and Cufflinks. HTseq was used to count the gene and lncRNA counts. The FPKM method was used to determine the gene

expression. We applied the DESeq algorithm to identify the differentially expressed genes. Significant analysis was performed using the *P*-value and false discovery rate (FDR) analysis. Differentially expressed genes were considered as those with a fold change >2 or fold change <0.5, FDR <0.05. GO analysis was performed to elucidate the biological implications of the differentially expressed genes, including biological process (BP), cellular component (CC), and molecular function (MF). GO annotations from NCBI (http://www.ncbi.nlm.nih.gov/), UniProt (http://www. uniprot.org/), and Gene Ontology (http://www.geneontology.org/) were downloaded. Pathway analysis was used to identify the significantly influenced pathways in which the differentially expressed genes were affected according to the Kyoto Encyclopedia of Genes and Genomes (KEGG) database. Fisher's exact test was used to identify the significantly influenced GO categories and pathways. The threshold of significance was defined by the *P* value.

Filipin staining for chondrocyte cholesterol assay

Cholesterol in chondrocytes was stained using the Cell Cholesterol Filipin Staining Kit (GMS80059.1; GenMed Scientifics, USA) according to the manufacturer' s instructions. Briefly, rat chondrocytes were washed with PBS, fixed in 10% neutral-buffered formalin for 10 min at 21℃, and then incubated with Filipin Staining solution for 30 min at 21℃ in the dark. After washing three times with PBS, the chondrocytes were observed using a confocal microscope (Olympus Life Science).

Co-immunoprecipitation

For co-immunoprecipitation assays, after chondrocytes transfected with Lv-Sdc4 (MOI=100) to overexpress SDC4 were lysed with cold RIPA lysis buffer. Lysates centrifuged at 12000 rpm for 10 min, and the supernatants were collected. Supernatants containing proteins were then incubated with 1 μg anti-SDC4 (PA1-32485; Invitrogen, USA), or 1 μg normal rabbit IgG (ab172730; Abcam) antibody overnight at 4 °C. Protein lysates were subsequently incubated with 20 μL pre-washed protein A/G PLUS-Agarose beads (sc-2003; Santa Cruz Biotechnology, USA) with gentle rotation for 3 h at 4 °C. The immunoprecipitates were then analysed by western blotting as described above using primary antibodies against ADAMT-5 (ab41037; Abcam) to detect SDC4 protein.

Statistical analysis

All statistical analyses were performed using SPSS (version 20.0; IBM Corp, Chicago, IL, USA). Data are presented as mean ± standard deviation. The Shapiro–Wilk test for normality, Levene's test for homogeneity of variance, and Student's t-test were performed to compare two independent groups. Multiple comparisons were performed using the Shapiro–Wilk test, Levene's test, and one-way analysis of

variance (ANOVA) with a post-hoc Bonferroni test. n indicates the number of biologically independent samples. Significant data are indicated by *P < 0.05; **P < 0.01; and ***P < 0.001.

Declarations

Data availability

All data in our study are available upon request. Source data are provided with this paper.

Acknowledgments

This work was supported by National Natural Science Foundation of China (NO. 82072486, NO. 81972101 and NO. 82002346). We would like to acknowledge Dr. Shan Wang, Dr. Tong Wu, Dr. Wenqiang Yan, Dr. Junyan Wang, La Li Ph.D. and Muyang Sun Ph.D. at Peking University Third Hospital for experimental technical guidance. We would also like to thank Editage (www.editage.com) for English language editing.

Author contributions

CXC conducted the majority of the experiments and completed the manuscript. YYS participated in the experiment and helped with manuscript preparation. YFA, XQH and JC conceived the project and designed the experiments. XZ, QL and JHZ helped perform the animal surgery. FYZ and QYM collected the clinical specimens. WLD and ZLL collected animal samples and scoring. JYZ, XF and JYZ revised the manuscript. YFA and XQH supervised the project. CXC and YYS contributed equally in this work.

Competing interests

The authors declare that they have no competing interests.

References

1. Hunter DJ, Bierma-Zeinstra S. Osteoarthritis. *Lancet* **393**, 1745-1759 (2019).

2. Jeon OH*, et al.* Local clearance of senescent cells attenuates the development of post-traumatic osteoarthritis and creates a pro-regenerative environment. *Nat Med* **23**, 775-781 (2017).

3. Englund M, Roemer FW, Hayashi D, Crema MD, Guermazi A. Meniscus pathology, osteoarthritis and the treatment controversy. *Nat Rev Rheumatol* **8**, 412-419 (2012).

4. Reeves ND, Bowling FL. Conservative biomechanical strategies for knee osteoarthritis. *Nat Rev Rheumatol* **7**, 113-122 (2011).

5. Courties A, Sellam J, Berenbaum F. Metabolic syndrome-associated osteoarthritis. *Curr Opin Rheumatol* **29**, 214-222 (2017).

6. Al-Arfaj AS. Radiographic osteoarthritis and serum cholesterol. *Saudi Med J* **24**, 745-747 (2003).

7. Villalvilla A, Gomez R, Largo R, Herrero-Beaumont G. Lipid transport and metabolism in healthy and osteoarthritic cartilage. *Int J Mol Sci* **14**, 20793-20808 (2013).

8. Mishra R*, et al.* A comparative analysis of serological parameters and oxidative stress in osteoarthritis and rheumatoid arthritis. *Rheumatol Int* **32**, 2377-2382 (2012).

9. Oliviero F*, et al.* A comparative study of serum and synovial fluid lipoprotein levels in patients with various arthritides. *Clin Chim Acta* **413**, 303-307 (2012).

10. Courties A, Berenbaum F, Sellam J. The Phenotypic Approach to Osteoarthritis: A Look at Metabolic Syndrome-Associated Osteoarthritis. *Joint Bone Spine* **86**, 725-730 (2019).

11. Tolleshaug H, Goldstein JL, Schneider WJ, Brown MS. Posttranslational processing of the LDL receptor and its genetic disruption in familial hypercholesterolemia. *Cell* **30**, 715-724 (1982).

12. Croy JE, Shin WD, Knauer MF, Knauer DJ, Komives EA. All three LDL receptor homology regions of the LDL receptor-related protein bind multiple ligands. *Biochemistry* **42**, 13049-13057 (2003).

13. Krieger M, Herz J. Structures and functions of multiligand lipoprotein receptors: macrophage scavenger receptors and LDL receptor-related protein (LRP). *Annu Rev Biochem* **63**, 601-637 (1994).

14. Lara-Castillo N, Johnson ML. LRP receptor family member associated bone disease. *Rev Endocr Metab Disord* **16**, 141-148 (2015).

15. Smith AJ*, et al.* Haplotypes of the low-density lipoprotein receptor-related protein 5 (LRP5) gene: are they a risk factor in osteoarthritis? *Osteoarthritis Cartilage* **13**, 608-613 (2005).

16. Shin Y*, et al.* Low-density lipoprotein receptor-related protein 5 governs Wnt-mediated osteoarthritic cartilage destruction. *Arthritis Res Ther* **16**, R37 (2014).

17. Joiner DM, Less KD, Van Wieren EM, Hess D, Williams BO. Heterozygosity for an inactivating mutation in low-density lipoprotein-related receptor 6 (Lrp6) increases osteoarthritis severity in mice after ligament and meniscus injury. *Osteoarthritis Cartilage* **21**, 1576-1585 (2013).

18. Ishii H, Kim DH, Fujita T, Endo Y, Saeki S, Yamamoto TT. cDNA cloning of a new low-density lipoprotein receptor-related protein and mapping of its gene (LRP3) to chromosome bands 19q12-q13. 2. *Genomics* **51**, 132-135 (1998).

19. Poole AR*, et al.* Proteolysis of the collagen fibril in osteoarthritis. *Biochem Soc Symp*, 115-123 (2003).

20. Stanton H*, et al.* ADAMTS5 is the major aggrecanase in mouse cartilage in vivo and in vitro. *Nature* **434**, 648-652 (2005).

21. Echtermeyer F*, et al.* Syndecan-4 regulates ADAMTS-5 activation and cartilage breakdown in osteoarthritis. *Nat Med* **15**, 1072-1076 (2009).

22. Binch ALA, Shapiro IM, Risbud MV. Syndecan-4 in intervertebral disc and cartilage: Saint or synner? *Matrix Biol* **52-54**, 355-362 (2016).

23. Chen H*, et al.* Electroacupuncture serum inhibits TNFalphamediated chondrocyte inflammation via the RasRafMEK1/2ERK1/2 signaling pathway. *Mol Med Rep* **16**, 5807-5814 (2017).

24. Bollmann M*, et al.* MMP-9 mediated Syndecan-4 shedding correlates with osteoarthritis severity. *Osteoarthritis Cartilage*, (2020).

25. Dahaghin S, Bierma-Zeinstra SM, Ginai AZ, Pols HA, Hazes JM, Koes BW. Prevalence and pattern of radiographic hand osteoarthritis and association with pain and disability (the Rotterdam study). *Ann Rheum Dis* **64**, 682-687 (2005).

26. Niu J, Clancy M, Aliabadi P, Vasan R, Felson DT. Metabolic Syndrome, Its Components, and Knee Osteoarthritis: The Framingham Osteoarthritis Study. *Arthritis Rheumatol* **69**, 1194-1203 (2017).

27. Onuora S. Osteoarthritis: Metabolic syndrome and risk of knee OA. *Nat Rev Rheumatol* **13**, 257 (2017).

28. Zhou M*, et al.* The cross-sectional and longitudinal effect of hyperlipidemia on knee osteoarthritis: Results from the Dongfeng-Tongji cohort in China. *Sci Rep* **7**, 9739 (2017).

29. Li H, George DM, Jaarsma RL, Mao X. Metabolic syndrome and components exacerbate osteoarthritis symptoms of pain, depression and reduced knee function. *Ann Transl Med* **4**, 133 (2016).

30. Farnaghi S*, et al.* Protective effects of mitochondria-targeted antioxidants and statins on cholesterol-induced osteoarthritis. *FASEB J* **31**, 356-367 (2017).

31. Choi WS*, et al.* The CH25H-CYP7B1-RORalpha axis of cholesterol metabolism regulates osteoarthritis. *Nature* **566**, 254-258 (2019).

32. Gierman LM*, et al.* Osteoarthritis development is induced by increased dietary cholesterol and can be inhibited by atorvastatin in APOE*3Leiden.CETP mice--a translational model for atherosclerosis. *Ann Rheum Dis* **73**, 921-927 (2014).

33. Clockaerts S*, et al.* Statin use is associated with reduced incidence and progression of knee osteoarthritis in the Rotterdam study. *Ann Rheum Dis* **71**, 642-647 (2012).

34. Arkill KP, Winlove CP. Fatty acid transport in articular cartilage. *Arch Biochem Biophys* **456**, 71-78 (2006).

35. Georgi N*, et al.* Differentiation of mesenchymal stem cells under hypoxia and normoxia: lipid profiles revealed by time-of-flight secondary ion mass spectrometry and multivariate analysis. *Anal Chem* **87**, 3981-3988 (2015).

36. de Munter W*, et al.* Cholesterol accumulation caused by low density lipoprotein receptor deficiency or a cholesterol-rich diet results in ectopic bone formation during experimental osteoarthritis. *Arthritis Res Ther* **15**, R178 (2013).

37. Jeong YH*, et al.* Molecular characterization and expression of the low-density lipoprotein receptor-related protein-10, a new member of the LDLR gene family. *Biochem Biophys Res Commun* **391**, 1110-1115 (2010).

38. Elsafadi M*, et al.* MicroRNA-4739 regulates osteogenic and adipocytic differentiation of immortalized human bone marrow stromal cells via targeting LRP3. *Stem Cell Res* **20**, 94-104 (2017).

39. Barre PE, Redini F, Boumediene K, Vielpeau C, Pujol JP. Semiquantitative reverse transcription-polymerase chain reaction analysis of syndecan-1 and -4 messages in cartilage and cultured chondrocytes from osteoarthritic joints. *Osteoarthritis Cartilage* **8**, 34-43 (2000).

40. Wang J, Markova D, Anderson DG, Zheng Z, Shapiro IM, Risbud MV. TNF-alpha and IL-1beta promote a disintegrin-like and metalloprotease with thrombospondin type I motif-5-mediated aggrecan degradation through syndecan-4 in intervertebral disc. *J Biol Chem* **286**, 39738-39749 (2011).

Figures

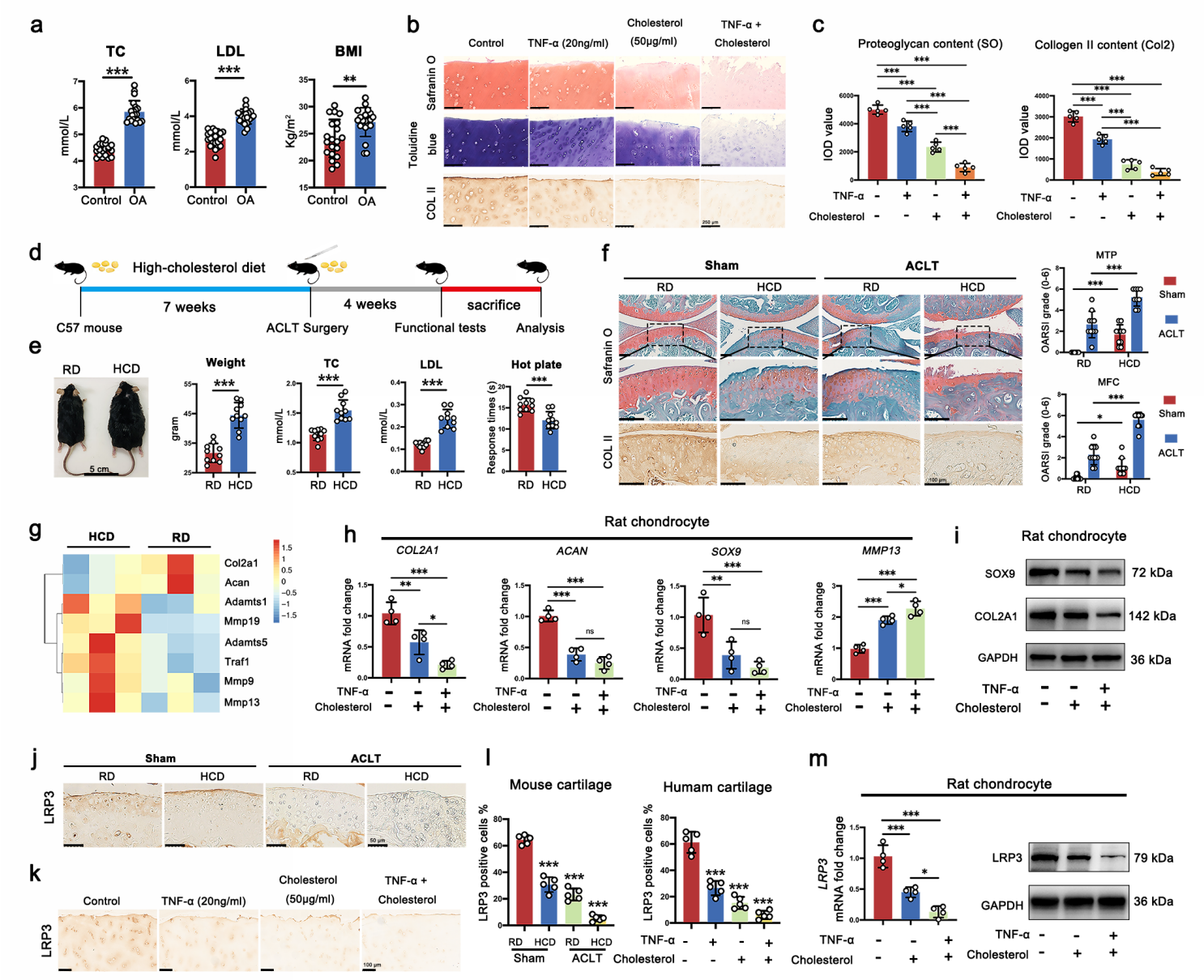

Figure 1

High cholesterol aggravates OA cartilage degeneration and downregulates the expression of LRP3 in cartilage. a Levels of serum total cholesterol (TC), low-density lipoprotein (LDL) and body mass index (BMI) in OA or meniscal injured (as control) patients (n = 20). b Safranin-O, toluidine blue and type II collagen immunohistochemistry (IHC) staining in human cartilage explants treated with cholesterol (50

μg/ml) and/or TNF-α (20 ng/ml) for 14 d. c The integrated optical density (IOD) value for proteoglycan content and type II collagen (COLII) determined by safranin O and immunohistochemistry staining (n = 5). d Scheme of the high-cholesterol diet (HCD) feeding and ACLT surgery in mice. e The general view, body weight, serum TC, serum LDL and pain response times of HCD mice compared with RD mice. f Representative images of safranin O-fast green, IHC staining of COLII, and the corresponding Osteoarthritis Research Society International (OARSI) scores from HCD mice and RD mice subjected to Sham or ACLT operation for 4 weeks. g Heatmap of mRNA-seq analysis in cartilage tissue of HCD and RD mice. h Quantification of mRNA levels for COL2A1, ACAN, SOX9 and MMP13 in rat chondrocytes treated with cholesterol (50 μg/ml) and/or TNF-α (20 ng/ml) for 3d (n = 4). i The proteins levels of SOX9 and COL2A1 in rat chondrocytes treated with cholesterol (50 μg/ml) and/or TNF-α (20 ng/ml) for 5d. j IHC staining for LRP3 in HCD mice and RD mice subjected to Sham or ACLT operation. k IHC staining for LRP3 in human cartilage explants treated with cholesterol (50 μg/ml) and/or TNF-α (20 ng/ml). l Quantification of LRP3-positive cells in mouse and human knee joint cartilage tissues (n = 5). m Quantification of LRP3 mRNA and proteins levels in rat chondrocytes treated with cholesterol (50 μg/ml) and/or TNF-α (20 ng/ml). Data are shown as the mean ± SD. *P < 0.05; **P < 0.01; ***P < 0.001.

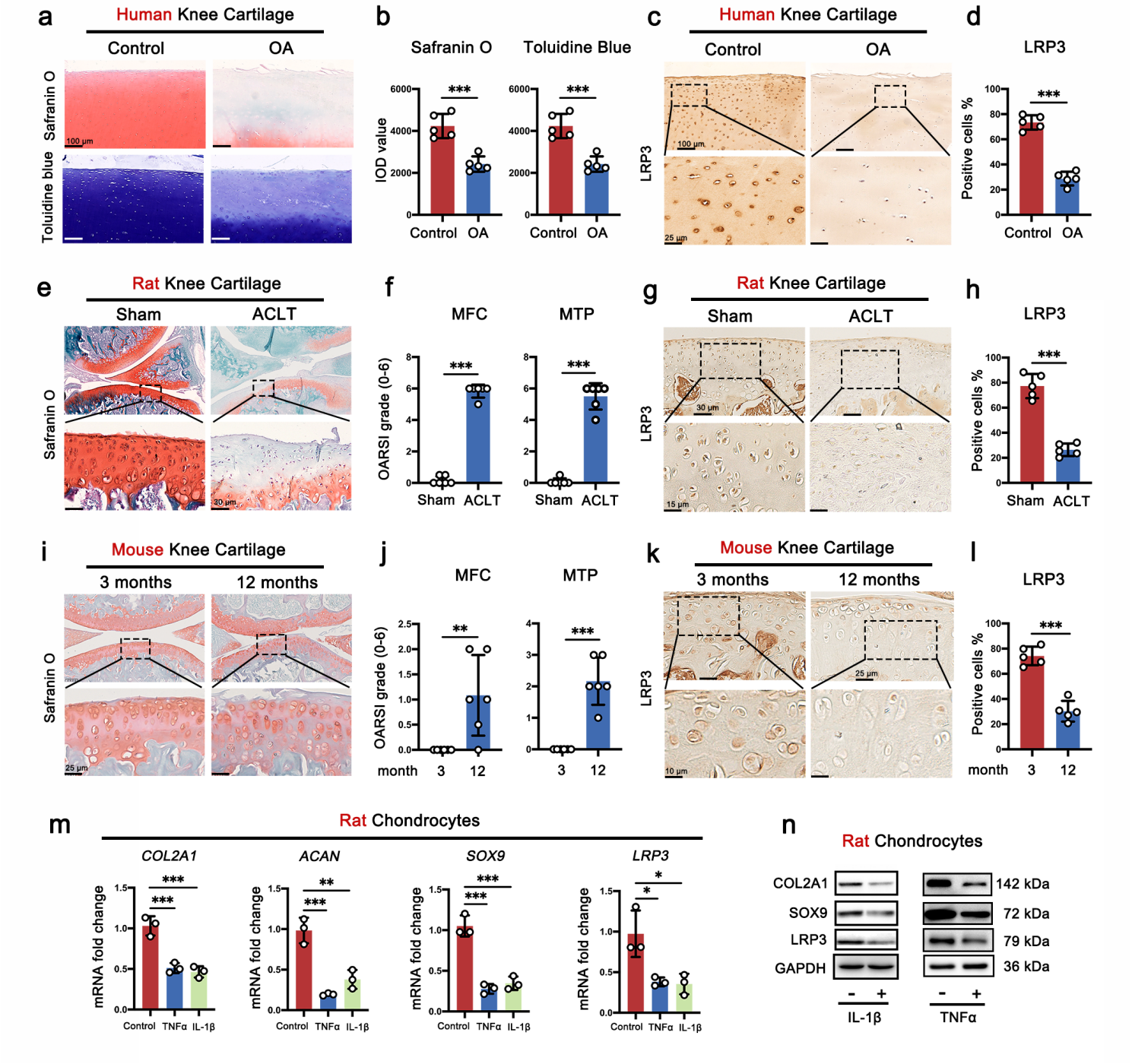

Figure 2

The expression of LRP3 is decreased during OA development. a Safranin-O and toluidine blue staining in human OA and normal cartilage tissue. b The IOD value for human cartilage proteoglycan content determined by safranin O and toluidine blue staining (n = 5). c IHC staining for LRP3 in human OA and normal cartilage, insets indicate the regions shown in the enlarged images. d Quantification of LRP3-positive cells in human OA and normal cartilage (n = 5). e Representative images of safranin O-fast green staining in rat Sham and ACLT knee cartilage, insets indicate the regions shown in the enlarged images. f OARSI scores of rat Sham and ACLT knee cartilage. g IHC staining for LRP3 in rat Sham and ACLT tibial

cartilage, insets indicate the regions shown in the enlarged images. h Quantification of LRP3-positive cells in rat Sham and ACLT tibial cartilage (n = 5). i Representative images of safranin O-fast green staining in 3 months and 12 months mouse knee cartilage, insets indicate the regions shown in the enlarged images. j OARSI scores of 3 months and 12 months mouse knee cartilage. k IHC staining for LRP3 in 3 months and 12 months mouse tibial cartilage, insets indicate the regions shown in the enlarged images. l Quantification of LRP3-positive cells in 3 months and 12 months mouse tibial cartilage (n = 5). m Quantification of mRNA levels for COL2A1, ACAN, SOX9 and LRP3 in rat chondrocytes treated with IL-1β (10 ng/ml) and TNF-α (20 ng/ml) for 3d (n = 3). n The proteins levels of SOX9, COL2A1 and LRP3 in rat chondrocytes treated with IL-1β (10 ng/ml) and TNF-α (20 ng/ml) for 5d. Data are shown as the mean ± SD. *P < 0.05; **P < 0.01; ***P < 0.001.

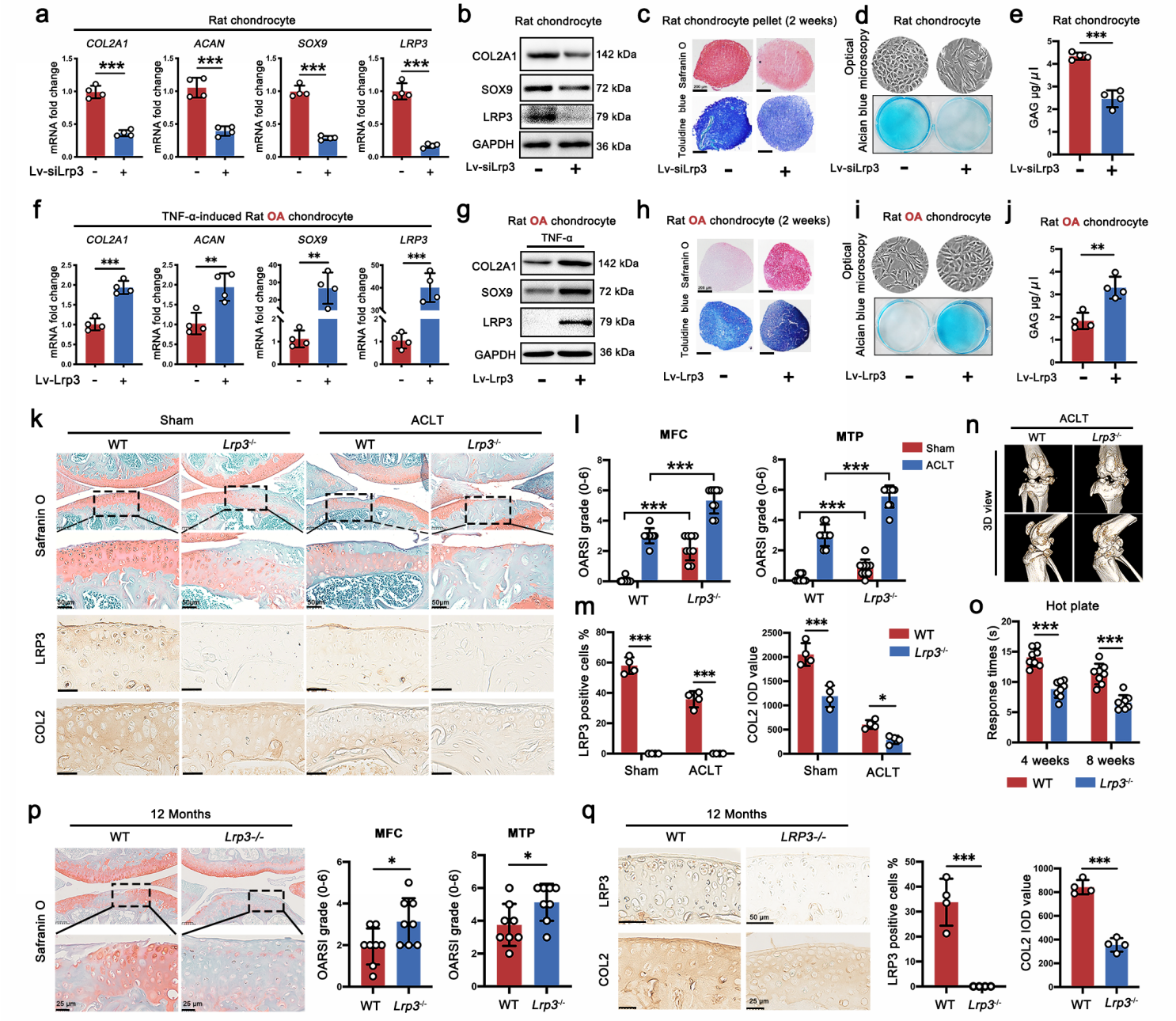

Figure 3

LRP3 positively regulates the metabolism of chondrocytes ECM and the deficiency of LRP3 aggravates the degeneration of knee joint cartilage. a Quantification of mRNA levels in rat chondrocytes treated with Lv-con313 (n = 4). b The proteins levels in rat chondrocytes treated with Lv-con313. c Safranin O and toluidine blue staining of rat chondrocyte pellets treated with Lv-con313 (n = 3). d Optical microscopy, alcian blue staining and (e) DMMB assays to examine to examine the effects of LRP3 knockdown on glycosaminoglycan expression in rat chondrocytes. f Quantification of mRNA levels in TNF-α (20 ng/ml)-induced rat OA chondrocytes treated with Lv-con335 (n = 4). g The proteins levels in TNF-α (20 ng/ml)-induced rat OA chondrocytes treated with Lv-con335. h Safranin O and toluidine blue staining of TNF-α (20 ng/ml)-induced rat OA chondrocyte pellets treated with Lv-con313 (n = 3). i Optical microscopy, alcian blue staining and (j) DMMB assays to examine the effects of LRP3 overexpression on glycosaminoglycan expression in TNF-α (20 ng/ml)-induced rat OA chondrocytes. k Representative images of safranin O-fast green, LRP3 and COLII IHC staining of knee joints from WT mice and Lrp3-/- mice subjected to Sham or ACLT operation for 8 weeks. l OARSI scores of WT mice and Lrp3-/- mice subjected to Sham or ACLT operation for 8 weeks (n = 9). m Quantification of LRP3-positive cells and IOD value for COLII in WT mice and Lrp3-/- mice subjected to Sham or ACLT operation for 8 weeks (n = 4). n Representative 3D view images of micro-CT of WT mice and Lrp3-/- mice subjected to ACLT operation for 8 weeks. o Pain response times when WT mice or Lrp3-/- mice were placed on the 55 °C hot plate meter at 4 w and 8 w post-surgery (n = 8). p Representative images of safranin O-fast green and OARSI scores of 12 months WT mice and Lrp3-/- mice. q LRP3 and COLII IHC staining of 12 months WT mice and Lrp3-/- mice. Data are shown as the mean ± SD. *P < 0.05; **P < 0.01; ***P < 0.001.

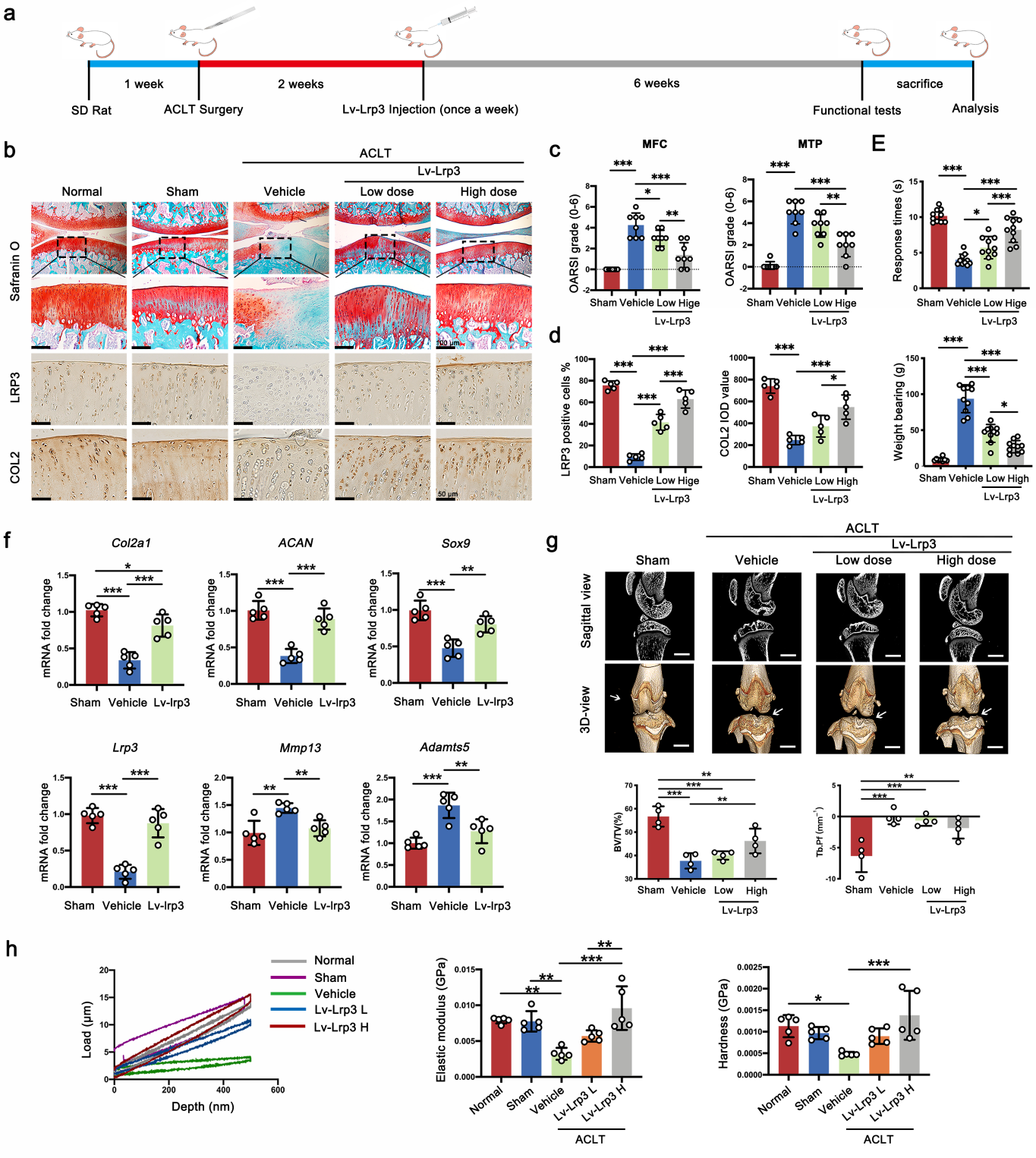

Figure 4

Overexpression of LRP3 in cartilage attenuates OA progression. a Scheme of the OA treatment with intra-articular injection of Lv-Lrp3 in rats. b Representative images of safranin O-fast green, COLII and LRP3 IHC staining, and (c) corresponding OARSI scores of Normal, Sham, Vehicle and Lv-Lrp3 treatment rats at 6 w, insets indicate the regions shown in the enlarged images. d Quantification of LRP3-positive cells and IOD value for COLII in Normal, Sham, Vehicle and Lv-Lrp3 treatment rats. e The pain response of rats was

analyzed using hot plate and weight bearing tests. f Quantification of mRNA levels for Col2a1, ACAN, Sox9, Lrp3, Mmp13 and Adamts5 in articular cartilage obtained from Sham, Vehicle and Lv-Lrp3(high dose group) treatment rats (n = 5). g Micro-CT Sagittal and 3D view and the quantitative micro-CT analysis of tibial subchondral bone with trabecular bone volume per total volume (BV/TV) and trabecular bone pattern factor (Tb. Pf) in Sham, Vehicle and Lv-Lrp3(high dose group) treatment rats (n = 4). h Biomechanical properties of cartilage samples from Normal, Sham, Vehicle and Lv-Lrp3 treatment rats at 6 w assessed using a nanoindentation test (n = 5). Data are shown as the mean ± SD. *P < 0.05; **P < 0.01; ***P < 0.001.

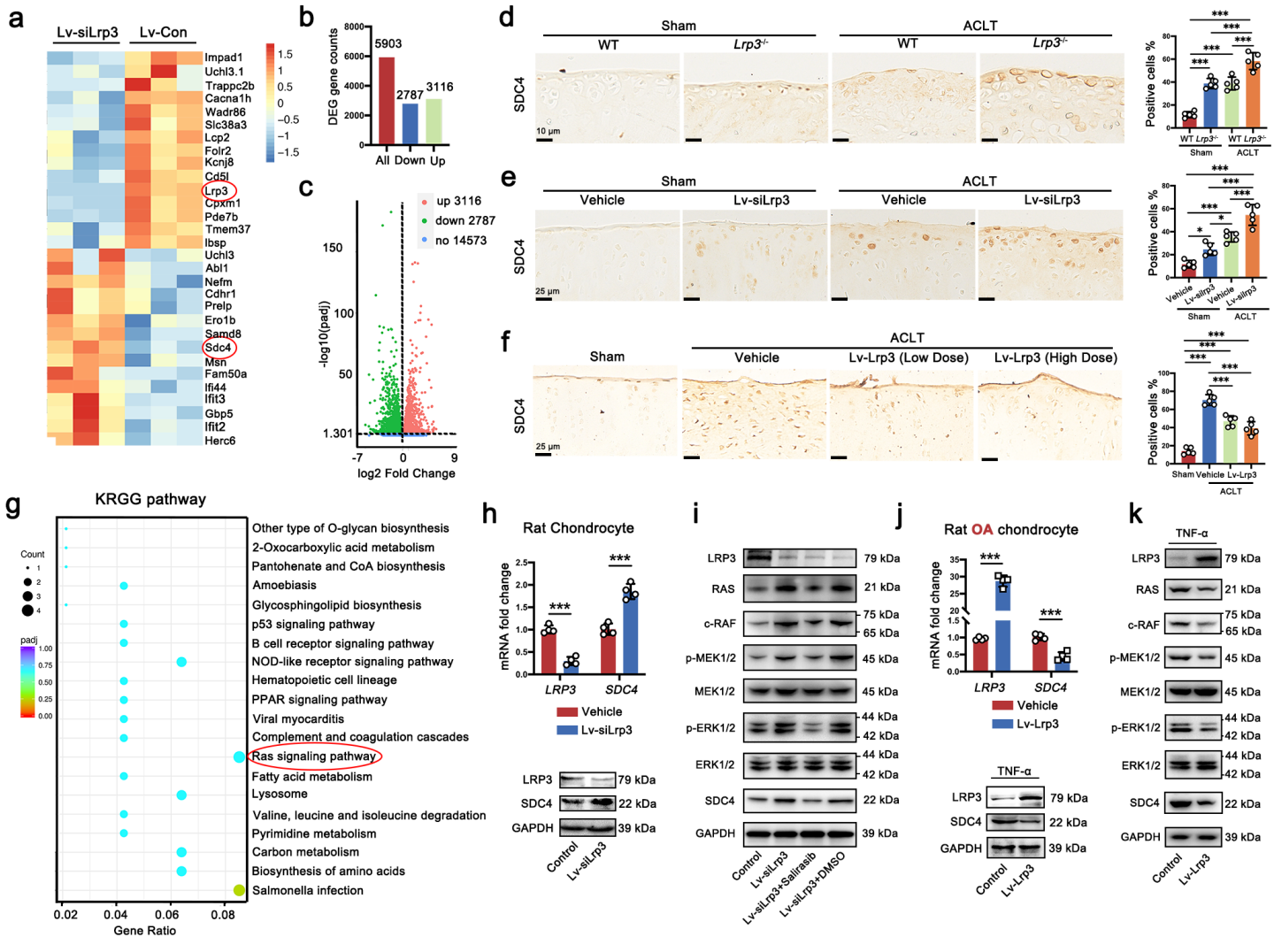

Figure 5

Knockdown of LRP3 up-regulates the expression of SDC4 by activating the Ras/Raf/MEK/ERK signaling pathway in chondrocytes. a Heatmap of mRNA-seq analysis in rat chondrocytes treated with Lv-con 313 or Lv-siLrp3. b RNA-seq comparison revealed a total of 5930 genes expressed, of which 3116 genes were upregulated and 2787 genes were downregulated. c The volcano plot illustrating of differential genes from RNA-seq analysis. d Representative images of LRP3 IHC staining of knee joints from WT and LRP3-/- mice subjected to Sham or ACLT operation. e Representative images of LRP3 IHC staining of

knee joints from vehicle or Lv-siLrp3 injected rats subjected to Sham or ACLT operation. f Representative images of LRP3 IHC staining of knee joints from Sham, Vehicle and Lv-Lrp3 treatment rats. g KEGG pathway analysis of upregulated targets in LRP3-knockdown transcriptome. h Quantification of LRP3 and SDC4 mRNA and proteins levels in rat chondrocytes treated with Lv-con313 or Lv-siLrp3. i Western blot analysis of the Ras/Raf/MEK/ERK signaling pathway and SDC4 in rat chondrocytes treated with Lv-con313, Lv-siLrp3 and/or Salirasib. j Quantification of LRP3 and SDC4 mRNA and proteins levels in TNF-α (20 ng/ml)-induced rat OA chondrocytes treated with Lv-con335 or Lv-Lrp3. k Western blot analysis of the Ras/Raf/MEK/ERK signaling pathway and SDC4 in TNF-α (20 ng/ml)-induced rat OA chondrocytes treated with Lv-con335 or Lv-Lrp3. Data are shown as the mean ± SD. *P < 0.05; **P < 0.01; ***P < 0.001.

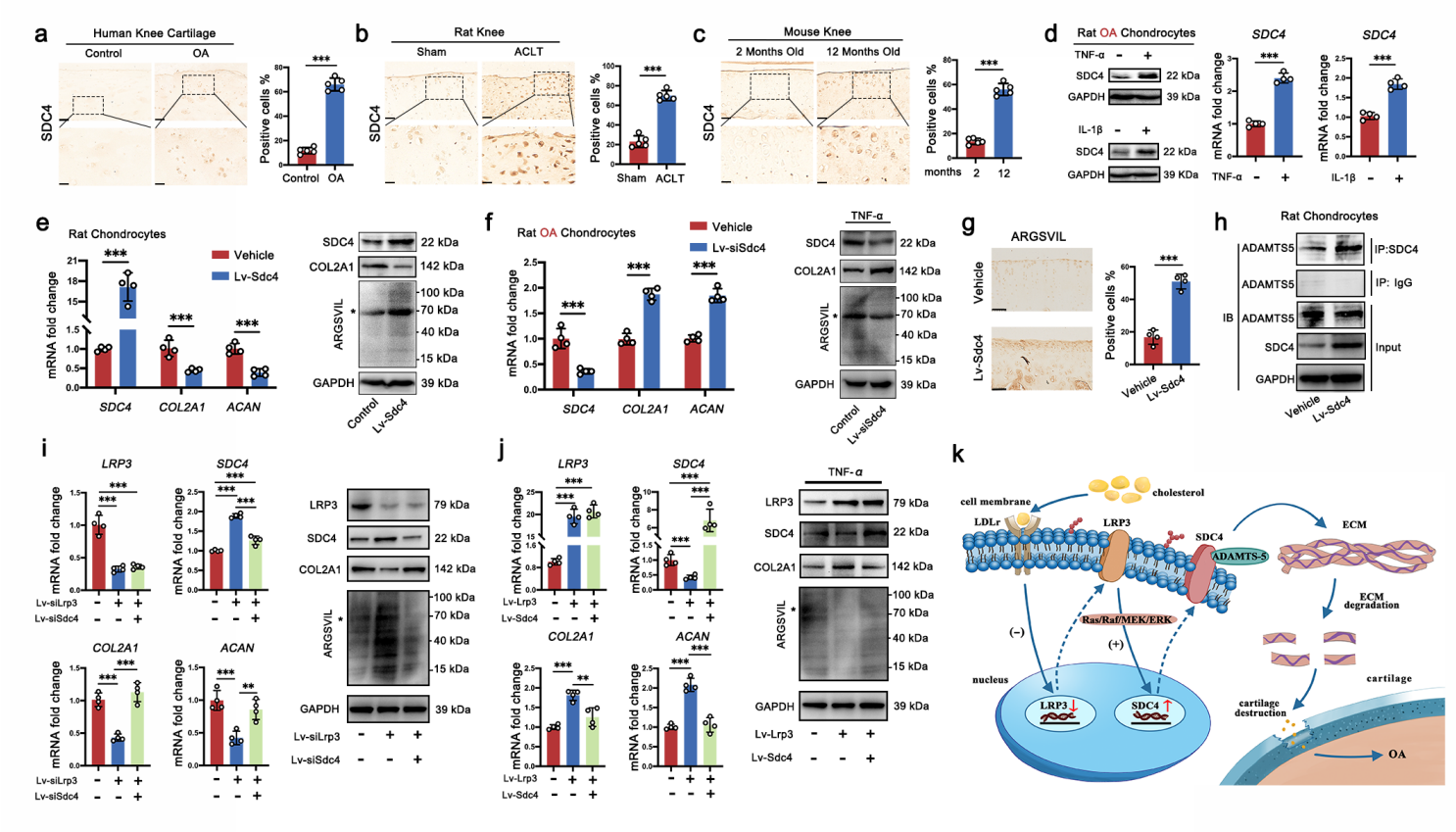

Figure 6

Identification of SDC4 as the downstream molecular targets of LRP3 in chondrocytes. a IHC staining for SDC4 in human OA and normal cartilage, insets indicate the regions shown in the enlarged images (n = 5). b IHC staining for SDC4 in rat Sham and ACLT tibial cartilage, insets indicate the regions shown in the enlarged images (n = 5). c IHC staining for SDC4 in 3 months and 12 months mouse tibial cartilage, insets indicate the regions shown in the enlarged images (n = 5). d Quantification of SDC4 mRNA and proteins levels in rat chondrocytes treated with IL-1β (10 ng/ml) and TNF-α (20 ng/ml) (n = 4). e Quantification of COL2A1, ACAN and SDC4 mRNA and proteins levels and aggrecan neoepitope (ARGSVIL) in rat chondrocytes treated with Lv-con 335 or Lv-Sdc4. f Quantification of COL2A1, ACAN and SDC4 mRNA and proteins levels and aggrecan neoepitope (ARGSVIL) in TNF-α (20 ng/ml)-induced rat OA chondrocytes treated with Lv-con 313 or Lv-siSdc4. g IHC staining for ARGSVIL in tibial cartilage of

vehicle or Lv-Sdc4 injected rats (n = 4). h The interaction of SDC4 and ADAMTS5 was verified by Co-immunoprecipitation (Co-IP) analysis. i Quantification of COL2A1, ACAN, LRP3 and SDC4 mRNA and proteins levels and ARGSVIL in rat chondrocytes treated with Lv-siLrp3 and Lv-siSdc4. j Quantification of COL2A1, ACAN, LRP3 and SDC4 mRNA and proteins levels and ARGSVIL in rat chondrocytes treated with Lv-Lrp3 and Lv-Sdc4. k Schematic of role of cholesterol-LRP3-SDC4 axis in pathogenesis of OA cartilage degeneration. Data are shown as the mean ± SD. *P < 0.05; **P < 0.01; ***P < 0.001.

Supplementary Files

This is a list of supplementary files associated with this preprint. Click to download.

- Rawdatainthemanuscript1.xlsx
- Rawdatainthemanuscript2.pdf
- SupplementaryFigures.docx